Nonequilibrium Longitudinal-Optical Phonon Effects in GaAs-AlGaAs Quantum Wells

P. Lugli
Dipartimento di Fisica, Università di Modena, 41100 Modena, Italy

and

S. M. Goodnick
Department of Electrical and Computer Engineering, Oregon State University, Corvallis, Oregon 97331

(Received 3 November 1986)

We use an ensemble Monte Carlo technique to study the electron and phonon dynamics in a single quantum well of GaAs-AlGaAs under optical excitation. The cooling of the photoexcited quasi two-dimensional electron distribution is studied in the presence of a nonequilibrium longitudinal-optical phonon population and electron-electron interaction. It is found that the presence of hot phonons due to emission from the photoexcited carriers in the quantum well reduces the electron relaxation rate in qualitative agreement with available experimental results in such systems.

PACS numbers: 73.40.Lq, 63.20.Kr, 72.20.Ht

Recent results from time-resolved studies of the hot-carrier relaxation in GaAs-AlGaAs quantum wells have shown that the relaxation times for photoexcited electrons are much longer than are expected from simple consideration of the bulk electron–longitudinal-optical (LO) phonon interaction.[1-3] Several possibilities have been suggested for this slow cooling rate: (i) enhanced screening of the electron–LO-phonon interaction due to the two-dimensional gas, (ii) reduction in the electron-phonon interaction due to confinement of the lattice modes in the quantum well, and (iii) the presence of a nonequilibrium population of LO phonons. Recent calculations of the effect of dynamical screening of the two-dimensional electron gas on the LO-phonon interaction[4] indicate a 50% reduction in the total scattering due to this effect. This is not enough in itself to account for the difference in relaxation rates observed experimentally. The existence of "slab" modes of the optical vibrations in confined systems has been studied by Riddoch and Ridley.[5] There it was shown that for wells larger than 150 Å, the difference in scattering rates between slab modes and bulk modes is fairly small. The presence of nonequilibrium hot phonons in bulk systems under high optical excitation has been shown from time-resolved Raman studies.[6] Their effect on the hot-carrier relaxation in bulk GaAs has been calculated analytically by Pötz and Kocevar[7] and found to explain retarded cooling effects observed experimentally in the bulk.[8] For quantum wells, Shah *et al.*[3] have argued that the effect of nonequilibrium phonons is the dominant effect contributing to slow carrier relaxation.

In the present study, we show the importance of nonequilibrium phonon effects in the cooling rates of photoexcited electrons in a quantum well through an ensemble Monte Carlo simulation discussed in detail elsewhere.[9] We consider a single quantum well of GaAs-$Al_{0.23}Ga_{0.77}As$ in our calculation, with the subband energies given by the solution of the one-dimensional square-well potential for a barrier height of 0.28 eV. The two-dimensional electrons are assumed to interact with unscreened bulk LO phonons. The reported effects of screening of the LO phonon interaction and the subsequent effect on cooling vary considerably in the literature both for the bulk and quantum wells and will not be considered here. The scattering rates for both intrasubband and intersubband transitions are calculated fully numerically, similar to other calculations of this mechanism for confined systems.[10,11] Intervalley transfer to the satellite L valleys ($E_{\Gamma L}=0.283$ eV) is included in the calculation where the L valleys are assumed quantized with the same barrier as the central valley. We have introduced two-dimensional electron-electron scattering into the Monte Carlo simulation through a generalization to multisubband systems of the self-scattering technique of Brunetti *et al.*[12] used for bulk Ge. Both intrasubband and intersubband scattering are considered, in which the various electrons are allowed to interact via a static screened Coulomb interaction determined by the long-wavelength limit of the two-dimensional Lindhard dielectric function at low temperature. In this approximation, the intersubband scattering rate is found to be negligible (intersubband in the sense that one of the participant electrons changes subbands after scattering), while the intrasubband rate (which includes scattering between electrons of different subbands) is at least an order of magnitude greater than the LO-phonon rate so that energy is exchanged between subbands allowing them to thermalize within a short time. Degeneracy in the quasi two-dimensional system is included through a generalization of the self-scattering technique proposed by Bosi and Jacoboni.[13,14] Electron-hole scattering has been neglected in this study. This effect may be important in the reported experiments, particularly at high excitation densities on undoped samples. For now we will concentrate on n-type samples with relatively low injection densities.

The nonequilibrium phonon distribution is given directly by a detailed balance of emission and absorption events during the simulation. On the time scales involved in the simulation, the group velocity of LO phonons is sufficiently small to neglect diffusion away from the well region. Because of confinement in the quantum well, there is not conservation of the component of the phonon wave vector q_z normal to the well. For an infinite well it has been shown[10] that the probability of scattering with a particular q_z is very peaked around momenta associated with the energy between the initial and final subband. Thus, for intrasubband scattering, phonons are emitted and absorbed with normal wave vectors close to zero, while intersubband events occur for $q_z \neq 0$. We assume that the overlap in momentum space of the various probabilities is small so that we may consider independent two-dimensional nonequilibrium phonon populations occurring for each q_z associated with each possible intersubband and intrasubband scattering event. For each value of q_z, the phonon population as a function of q (the magnitude of the parallel wave vector) is calculated and continually updated. The nonelectronic contributions (phonon-phonon and phonon-boundary scattering) are introduced via a phenomenological lifetime. No direct measurement of the LO-phonon lifetime in quantum-well systems is available at this time and thus a value of 7 ps is used here corresponding to the measured value for bulk GaAs at 77 K from Raman studies.[6] As the phonon population evolves in time, a self-scattering rejection technique is used to account for the modification of the scattering rate induced by the phonon perturbation.

The cooling of photoexcited electrons in n-type GaAs-AlGaAs quantum wells at low temperature (5 K) has been simulated. At each time step of the simulation (10 fs) carriers are added monoenergetically 0.25 eV above the lowest subband minima according to the generation rate of the laser pulse. The evolution in time of the generation rate is taken as an inverse hyperbolic cosine function of width 0.6 ps which peaks at 1 ps into the simulation. A cold background electron density of $2.5\times10^{11}/\mathrm{cm}^2$ is considered, similar to experimental studies on n-type samples.[3] Well widths of 50, 150, and 250 Å were considered with up to six subbands included (depending on the well width and height). Parameters for GaAs (including intervalley coupling constants) are essentially the same as used by Littlejohn, Hauser, and Glisson.[15]

Figure 1 shows the initial electron relaxation for an injected density of $5\times10^{11}/\mathrm{cm}^2$ and a 150-Å well width (four subbands allowed). The electron energy distribution function, $N(E)$, is plotted at different times during and after the laser excitation. The solid curve in the top figure represents the initial cold background electrons. At the maximum of the laser pulse ($t=1$ ps in this plot), a significant transfer of energy from the photoexcited electrons to the background electrons has already oc-

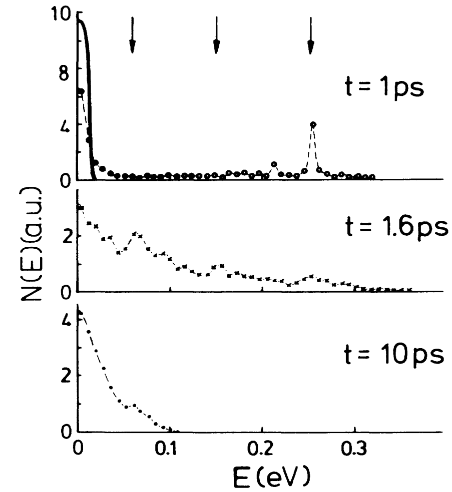

FIG. 1. Electron distribution function for various times before (solid curve), during (1 ps), and after (1.6, 10 ps) laser excitation. The arrows indicate the energy of higher subbands relative to the ground state.

curred. Furthermore, energy loss to the lattice through LO phonons has also occurred as shown by the secondary peak one phonon energy below the injection level. Shortly after the end of the pulse ($t=1.6$ ps), the strong intercarrier scattering creates a broad distribution where the subband minima (indicated by arrows) clearly appear. Within each subband, the distribution function starts to exhibit a Fermi-type appearance which is fully established at longer times as shown in the bottom curve. As a result of the spreading of the pulse arising from intercarrier scattering and hot phonons, a considerable number of electrons are excited above the minima of the satellite L valleys leading to intervalley transfer. This number depends strongly on the background density of cold carriers which absorb the energy of the high-energy injected electrons preventing transfer. For the densities considered here, typically 5%–15% of the injected electrons transfer within the first 4 ps of the simulation where they cool and retransfer back to the central valley within 10 ps. As the L-valley energy is close to that of the AlGaAs barrier, it is expected that a real-space transfer of carriers should occur as well. Although not modeled here, it is expected that the effect will be qualitatively the same as for intervalley transfer.

The electron relaxation towards equilibrium is accompanied by a buildup of the LO-phonon distribution due to the large energy loss via LO-phonon emission in the initial phase of the relaxation. Figure 2 shows the phonon distribution as a function of the phonon wave-vector component parallel to the well for $q_z=0$ at times during and after the laser pulse. For polar optical scattering, energy and momentum conservation set a lower limit on the parallel wave vector of the participating phonons which decreases with increasing electron energy [see, for

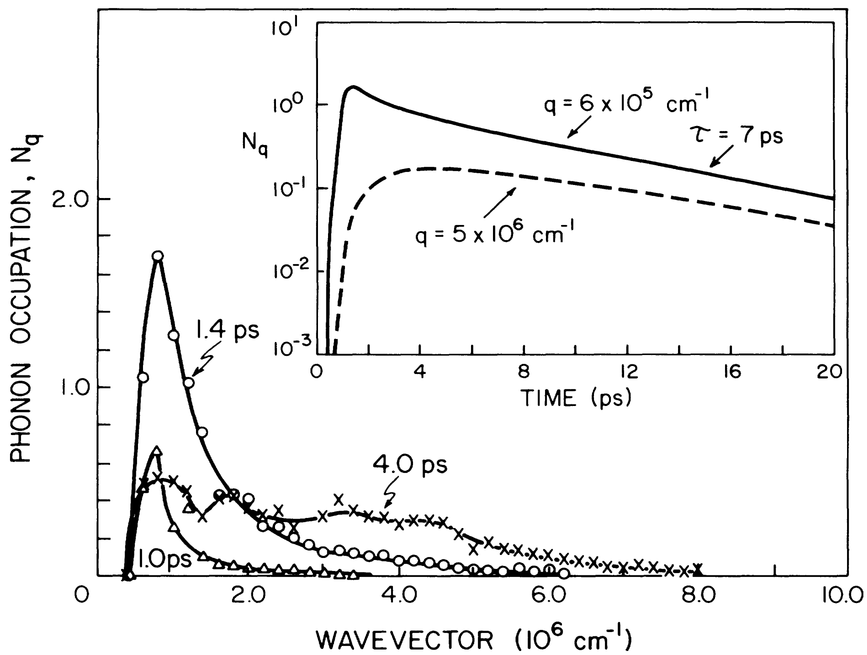

FIG. 2. Density of occupied phonon modes as a function of total parallel momentum for times during and after laser excitation for $q_z=0$ corresponding to intrasubband scattering. Inset: The decay vs time for $q=6\times10^5$ cm^{-1} (solid line) and $q=5\times10^6$ cm^{-1} (dashed curve).

example, Eq. (19) in Ref. 10]. For electrons injected at 0.25 eV, the minimum phonon wave vector for emission is 4.7×10^5 cm^{-1} which corresponds to the long-wavelength cutoff in the distribution of Fig. 2. The peak in the phonon distribution at $q=1\times10^6$ cm^{-1} corresponds to phonons emitted by the energetic photoinjected electrons during their initial relaxation. However, as the electrons thermalize through e-e scattering and phonon emission, phonons are emitted by electrons with energies close to the phonon emission threshold (35 meV). The minimum emitted phonon wave vector for electrons at this energy is 2.4×10^6 cm^{-1} and thus an increase in the nonequilibrium phonon population at longer times will occur at shorter wavelengths. This is evidenced in Fig. 2 for $t=4$ ps where a buildup of the phonon distribution around $q=4\times10^6$ cm^{-1} is observed. The minimum wave vector for phonon reabsorption also increases as the distribution cools which suggests that the population at small q as measured by Raman studies[6] is primarily governed by phonon relaxation and not by reabsorption. The inset in Fig. 2 shows the phonon population as a function of time for long-wavelength phonons ($q=6\times10^5$ cm^{-1}) and for phonons at $q=5\times10^6$ cm^{-1}. After a rapid initial decrease from the peak value, the long-wavelength population decreases with the 7-ps time constant assumed in the simulation as shown in the inset for $t>5$ ps. For the large-wave-vector population, the buildup in the distribution is delayed by several picoseconds in comparison, and the decay is slower because of continued emission, approaching the 7-ps rate at much longer times. For $q_z\neq0$ (corresponding to phonons generated through intersubband events), qualitatively similar behavior in the phonon population is found.

The induced LO-phonon perturbation feeds back into the electron system and is responsible for a reduction in the cooling rates, as shown in Fig. 3. There, the evolution of the average energy per electron (kinetic plus potential relative to the lowest subband) is presented as a function of time during and after the laser pulse. Note that the average energy may vary considerably from the electron temperature measured experimentally when the system is degenerate. If the phonons are forced to maintain an equilibrium distribution, the hot electrons are found to reach the equilibrium average energy shown by the dashed line in Fig. 3 (half of the Fermi energy at 5 K for a total concentration of 5×10^{11}/cm^2) in about 3 ps. A much slower relaxation is found when nonequilibrium phonons are accounted for, as shown by the two curves in Fig. 3, corresponding to two different injected densities of (2.5 and 5)$\times10^{11}$/cm^2. The reduction of the electron cooling rates is due to reabsorption of nonequilibrium phonons which build up at the earliest stages of the relaxation, as seen in Fig. 2. The effect is stronger when a considerable number of electrons have relaxed to the low-energy region below the emission threshold, resulting in the long-time tail in the average energy seen in Fig. 3. In this regime, the rates of LO-phonon emission and absorption are almost the same so that the energy loss rate is severely reduced. The decay rate in the average energy is thus dependent primarily on the phonon lifetime

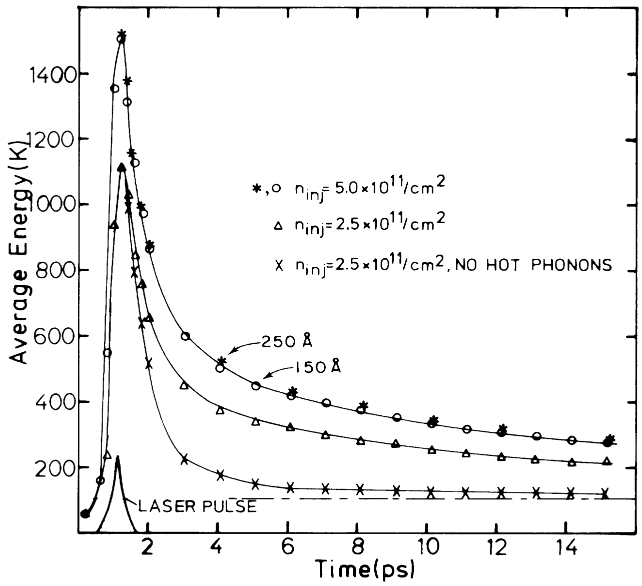

FIG. 3. Average total energy (kinetic plus potential) vs time for two different injection densities. The dashed curve represents the equilibrium energy at 5 K for a total carrier concentration of $5.0\times10^{11}/cm^2$. For $n_{inj}=5.0\times10^{11}/cm^2$, results are shown for well widths of 150 Å (circles) and 250 Å (asterisks).

and by variation of this parameter, proportional changes in the cooling are found in the results. A difference in the cooling between the two injection levels arises because more energy is pumped into the system at the higher injection density and thus a higher peak temperature is reached. The decay rate for the two curves in Fig. 3 is qualitatively the same since the energy loss is primarily governed by the phonon decay once the emission and absorption rates become comparable. However, at longer times when phonon reabsorption effects are strong, electron-hole scattering will reduce the energy by losses through transverse optical modes coupling to the holes,[7] increasing the cooling rate shown, especially at higher injection densities where the electron and hole concentrations are similar. This effect has not been studied in quantum-well systems and will be the subject of future work. As shown in Fig. 3, there is little difference between the cooling rate for a 150-Å (circles) well width and a 250-Å (asterisks) well (six subbands included) for the given injection level. The same result was found when a 50-Å well was considered. Experimentally, Ryan *et al.*[1] found differences between 150- and 250-Å wells in time-resolved experiments for times longer than 20 ps, which is longer than the time scale of Fig. 3. For longer times, other effects not considered here such as electron-hole interaction and recombination play an important role which could account for such differences.

We thank R. Brunetti, C. Jacoboni, and P. Kocevar for many useful discussions regarding this work. The authors acknowledge the support of IBM Corporation and the Alexander von Humboldt Foundation in making this work possible.

[1]J. F. Ryan, R. A. Taylor, A. J. Turberfield, and J. M. Worlock, Surf. Sci. **170**, 511 (1986).

[2]Z. Y. Xu and C. L. Tang, Appl. Phys. Lett. **44**, 692 (1984).

[3]J. Shah, A. Pinczuk, A. C. Gossard, and W. Wiegmann, Phys. Rev. Lett. **54**, 2045 (1985).

[4]S. Das Sarma, W. L. Lai, and X. C. Xie, in *Proceedings of the Eighteenth International Conference on the Physics of Semiconductors, Stockholm, Sweden, 1986,* edited by O. Engström (World Scientific, Singapore, 1987), p. 651.

[5]F. Riddoch and B. Ridley, Physica (Amsterdam) **134B**, 342 (1985).

[6]N. von der Linde, J. Kuhl, and H. Klingenburg, Phys. Rev. Lett. **44**, 1505 (1980).

[7]W. Pötz and P. Kocevar, Phys. Rev. B **28**, 7040 (1983).

[8]R. F. Leheny, J. Shah, R. F. Fork, C. V. Shank, and A. Migus, Solid State Commun. **31**, 809 (1979).

[9]S. M. Goodnick and P. Lugli, to be published.

[10]F. A. Riddoch and B. K. Ridley, J. Phys. C **16**, 6971 (1983).

[11]K. Yokoyama and K. Hess, Phys. Rev. B **31**, 6872 (1985).

[12]R. Brunetti, C. Jacoboni, A. Matulionis, and V. Dienys, Physica (Amsterdam) **134B**, 369 (1985).

[13]S. Bosi and C. Jacoboni, J. Phys. C **9**, 315 (1976).

[14]P. Lugli and D. K. Ferry, IEEE Trans. Electron Devices **32**, 2431 (1985).

[15]M. A. Littlejohn, J. R. Hauser, and T. H. Glisson, J. Appl. Phys. **48**, 4587 (1977).